Supplementary material for

Altitudinal variation in impacts of snow cover, reservoirs and precipitation seasonality on monthly runoff in Tibetan Plateau catchments

Nan Wu[a,b,c,f], Ke Zhang[a,b,c,d,e,*], Amir Naghibi[f], Hossein Hashemi[f], Zhongrui Ning[b,c], Jerker Jarsjö[g]

[a]*The National Key Laboratory of Water Disaster Prevention, Hohai University, Nanjing, Jiangsu, 210024, China*

[b]*Yangtze Institute for Conservation and Development, Hohai University, Nanjing, Jiangsu, 210024, China*

[c]*College of Hydrology and Water Resources, Hohai University, Nanjing, Jiangsu, 210024, China*

[d]*China Meteorological Administration Hydro-Meteorology Key Laboratory, Hohai University, Nanjing, Jiangsu, 210024, China*

[e]*Key Laboratory of Water Big Data Technology of Ministry of Water Resources, Hohai University, Nanjing, Jiangsu, 210024, China*

[f]*Division of Water Resources Engineering, LTH, Lund University, Lund, 22100, Sweden*

[g]*Department of Physical Geography, Stockholm University, Stockholm, 10691, Sweden;*

* Corresponding author at: The National Key Laboratory of Water Disaster Prevention, Hohai University, Nanjing, Jiangsu, 210098, China

E-mail address: kzhang@hhu.edu.cn (Ke Zhang)

The relative proportions of hydrological variables reflect their importance in hydrological processes, as shown in Figure S1. As both $\Delta S'$ and R exhibited negative values (Fig. 3), their absolute values were used in calculating the relative proportions, ensuring the relative proportions of P_r, S_{melt}, $\Delta S'$, R, and E summed up to 1. The proportion of P_r ($\frac{|P_r|}{|P_r| + |S_{melt}| + |\Delta S'| + |R| + |P_r|}$) increased from March to July, peaking at 50%, and decreased from August to November, with relative proportions in January, February, and December all below 6%. On the other hand, the relative proportion of $\Delta S'$ was higher from January to March and from November to February. S_{melt} primarily occurred in March and April, predominantly distributed in the GZ, ZB, DF, YJ, and ZS, with GZ having the highest proportion (44%). The relative proportions of R and E were generally greater than 10%, with the proportion of R being small from March to June, while E was prominent from February to May.

Figure Captions

Figure S1. Mean normalized monthly magnitude of the water balance term relative to the magnitude of all water balance terms, expressed as percentage from 0% (left part of grid cells, dark colors) to 100% (right, light).

Figure S2. Contribution box of different factors to R_v in 10 sub-basins, P_r, S_{melt}, $\Delta S'$ and E_0 represent rainfall, snowmelt, water storage change except snow, and potential evapotranspiration, respectively, P_r-S_{melt}, P_r-$\Delta S'$, P_r-E_0, S_{melt}-$\Delta S'$, S_{melt}-E_0, and E_0-$\Delta S'$ represent their covariance.

Figure S3. Relationship between the monthly ratio of water demand to water supply ($E/(P_r+S_{melt}-\Delta S')$) and monthly ratio of potential water demand to water supply ($E_0/(P_r+S_{melt}-\Delta S')$) in the representative basin (LN, YJ and ZS).

Table Captions

Table S1. Parameter n values for 10 sub-basins and the annual average evapotranspiration calculated based on the Budyko and extended Budyko framework.

Table S2. Location of outlet stations in 10 sub-basins and basic hydrological and meteorological information.

Table S3. The performance of extended Budyko framework in simulating evapotranspiration.

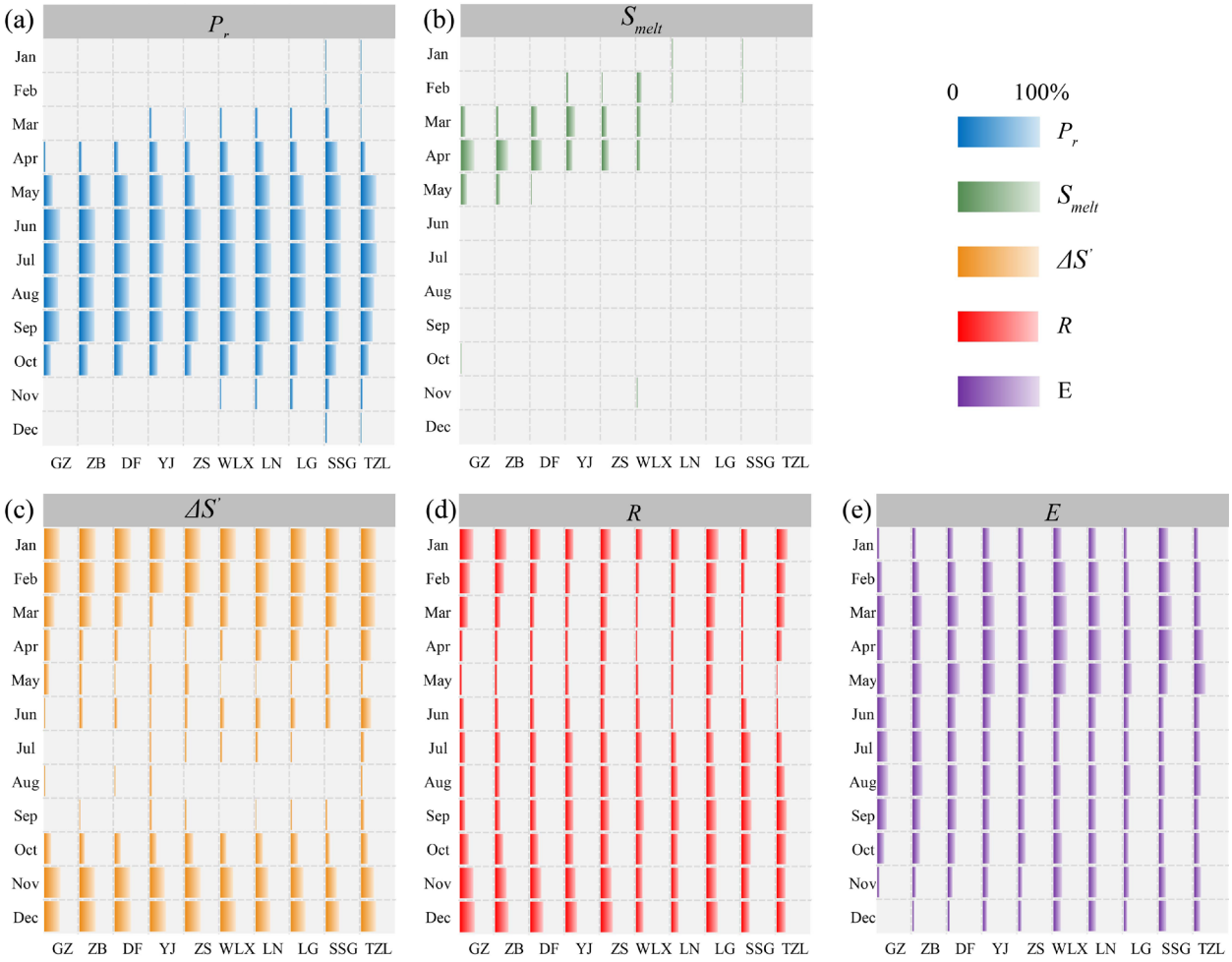

Figure S1. Mean normalized monthly magnitude of the water balance term relative to the magnitude of all water balance terms, expressed as percentage from 0% (left part of grid cells, dark colors) to 100% (right, light).

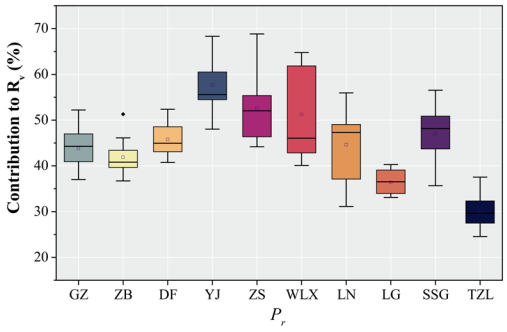
Contribution to R_v (%)
GZ ZB DF YJ ZS WLX LN LG SSG TZL
P_r

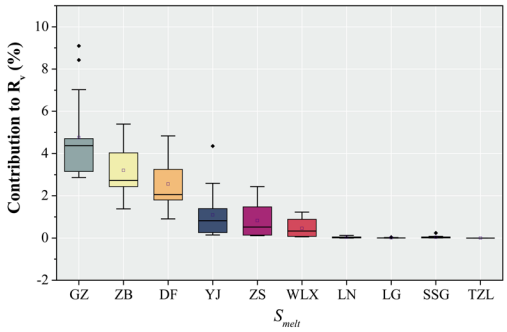
Contribution to R_v (%)
GZ ZB DF YJ ZS WLX LN LG SSG TZL
S_{melt}

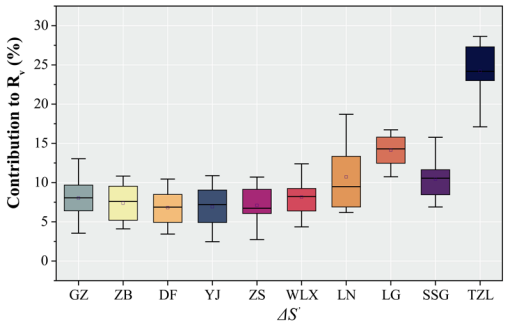
Contribution to R_v (%)
GZ ZB DF YJ ZS WLX LN LG SSG TZL
$\Delta S'$

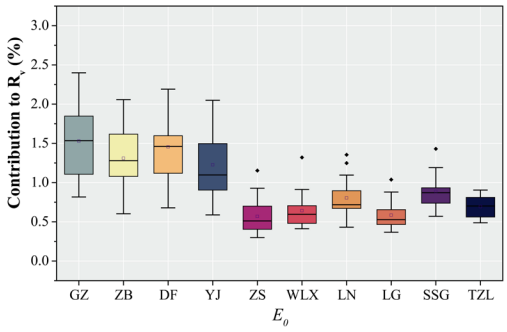
Contribution to R_v (%)
GZ ZB DF YJ ZS WLX LN LG SSG TZL
E_0

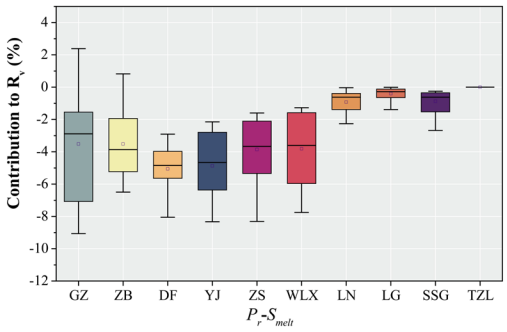
Contribution to R_v (%)
GZ ZB DF YJ ZS WLX LN LG SSG TZL
P_r-S_{melt}

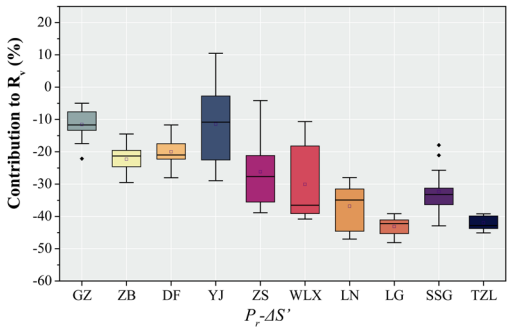
Contribution to R_v (%)
GZ ZB DF YJ ZS WLX LN LG SSG TZL
P_r-$\Delta S'$

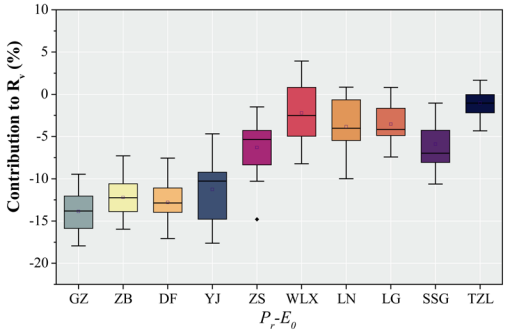
Contribution to R_v (%)
GZ ZB DF YJ ZS WLX LN LG SSG TZL
P_r-E_0

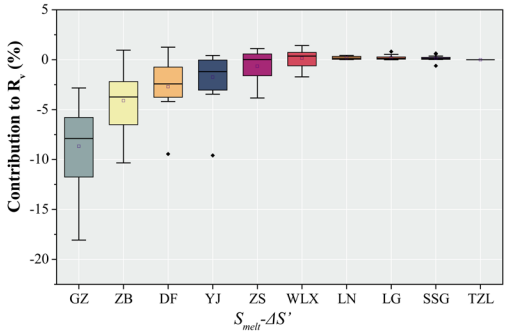
Contribution to R_v (%)
GZ ZB DF YJ ZS WLX LN LG SSG TZL
S_{melt}-$\Delta S'$

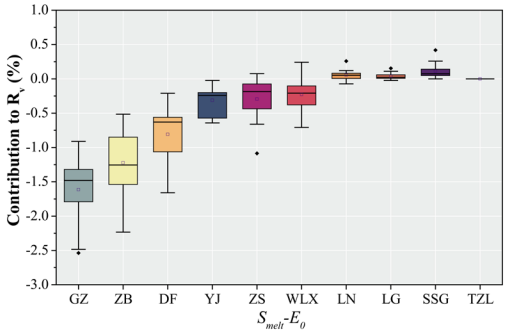
Contribution to R_v (%)
GZ ZB DF YJ ZS WLX LN LG SSG TZL
S_{melt}-E_0

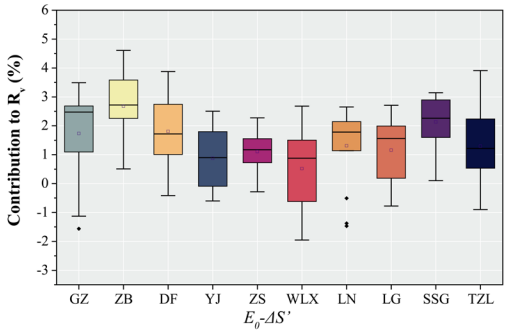
Contribution to R_v (%)
GZ ZB DF YJ ZS WLX LN LG SSG TZL
E_0-$\Delta S'$

Figure S2. Contribution box of different factors to R_v in 10 sub-basins, P_r, S_{melt}, $\Delta S'$ and E_0 represent rainfall, snowmelt, water storage change except snow, and potential evapotranspiration, respectively. P_r-S_{melt}, P_r-$\Delta S'$, P_r-E_0, S_{melt}-$\Delta S'$, S_{melt}-E_0, and E_0-$\Delta S'$ represent their covariance.

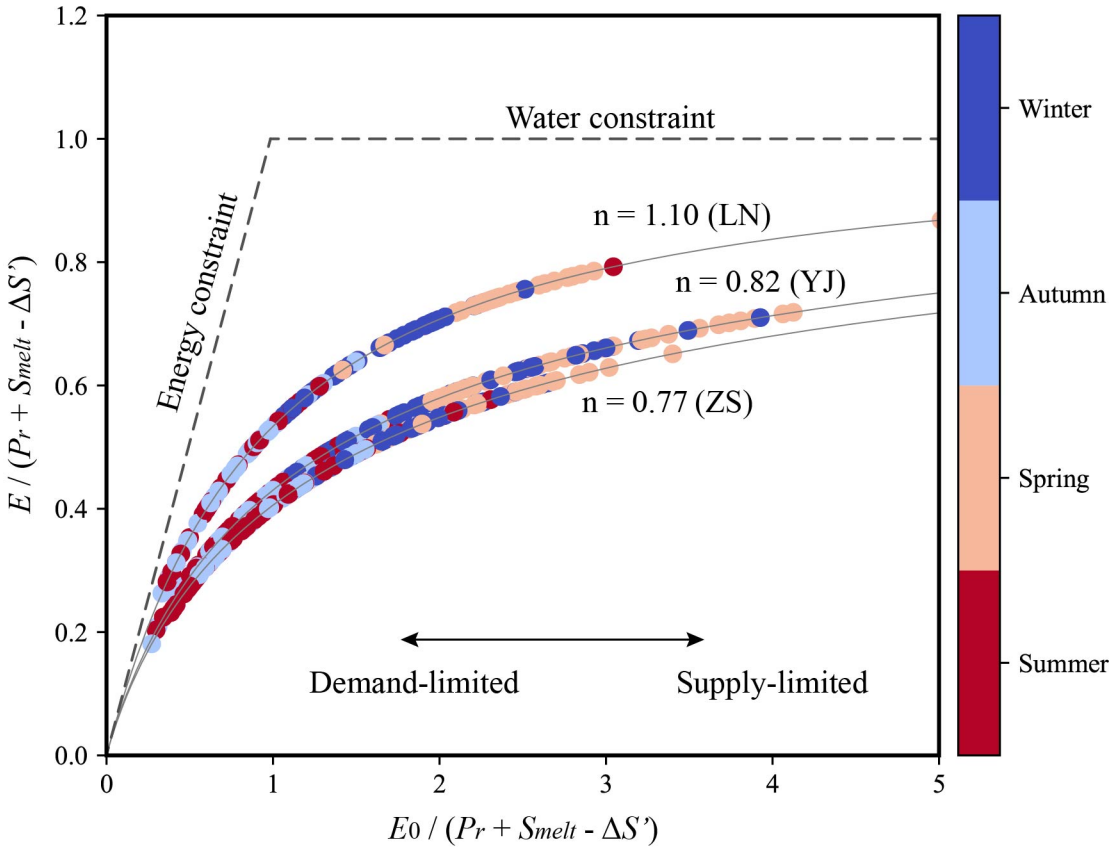

60

Figure S3. Relationship between the monthly ratio of water demand to water supply ($E/(P_r+S_{melt}-\Delta S')$) and monthly ratio of potential water demand to water supply ($E_0/(P_r+S_{melt}-\Delta S')$) in the representative basin (LN, YJ and ZS).

Table S1. Parameter *n* values for 10 sub-basins and the annual average evapotranspiration calculated based on the Budyko and extended Budyko framework.

Basin	GZ	ZB	DF	YJ	ZS	LN	WLX	LG	SSG	TZL
n	1.26	1.50	1.23	0.82	0.77	1.10	1.68	0.75	0.88	0.79
E_B (mm)	402	475	455	497	478	527	652	642	604	593
E_{EB} (mm)	425	479	440	479	442	508	634	706	575	560

Table S2. Location of outlet stations in 10 sub-basins and basic hydrological and meteorological information.

Number	Site Name	Abbreviation of subbasin	Latitude	Longitude	Area (million km^2)	Monthly Streamflow (mm)	Monthly Precipitation (mm)	Monthly Temperatures (℃)	Monthly Potential Evapotranspiration (mm)
1	Ganzi	GZ	31.62°	99.97°	3.27	21.45	54.74	-1.60	61.25
2	Zhuba	ZB	31.43°	100.68°	0.69	24.28	63.63	-0.45	62.75
3	Daofu	DF	31.03°	101.07°	0.73	28.88	66.22	0.73	66.69
4	Yajiang	YJ	30.03°	101.02°	1.89	40.96	70.92	2.18	73.47
5	Zhuosang	ZS	29.70°	100.38°	0.31	40.95	68.30	1.77	76.10
6	Luning	LN	28.45°	101.87°	3.64	38.73	80.87	5.95	81.93
7	Wulaxi	WLX	28.48°	101.65°	0.25	40.66	92.78	3.13	72.96
8	Lugu	LG	28.30°	102.18°	0.21	84.13	97.20	8.65	78.73
9	Sunshuiguan	SSG	28.30°	102.20°	0.16	55.74	94.93	10.25	81.66.
10	Tongzilin	TZL	26.68°	101.85°	1.65	62.31	91.58	13.29	99.47

Table S3. The performance of extended Budyko framework in simulating evapotranspiration.

Basin	GZ	ZB	DF	YJ	ZS	LN	WLX	LG	SSG	TZL
NSE	0.87	0.81	0. 90	0.93	0.87	0.86	0.93	0.90	0.89	0.82